

Are Pulsar Giant Pulses Induced by Re-emission of Cyclotron Resonance Absorption?

Ji-Guang Lu^{1,2}, Wei-Yang Wang^{3,4}, Bo Peng^{1,2}, Ren-Xin Xu^{5,6}

¹ CAS Key Laboratory of FAST, National Astronomical Observatories, Chinese Academy of Sciences, Beijing 100101, China; lujig@nao.cas.cn

² Guizhou Radio Astronomy Observatory, Chinese Academy of Sciences, Guiyang 550025, China;

³ Key Laboratory for Computational Astrophysics, National Astronomical Observatories, Chinese Academy of Sciences, 20A Datun Road, Beijing 100101, China;

⁴ University of Chinese Academy of Sciences, Beijing 100049, China

⁵ Department of Astronomy, Peking University, Beijing 100871, China;

⁶ Kavli Institute for Astronomy and Astrophysics

Abstract It is conjectured that coherent re-emission of cyclotron resonance absorption could result in pulsar giant pulses. This conjecture seems reasonable as it can naturally explain the distribution of pulsars with giant pulses on the P - \dot{P} diagram.

Key words: pulsars: general — radiation mechanisms: non-thermal — plasmas — magnetic fields

1 INTRODUCTION

Pulsars were discovered more than half a century ago, but their radiation mechanism, in both radio and X/γ -ray bands, remains uncertain. The coherent radio radiation of a pulsar is generated by charged particles (i.e., dense plasma) in its magnetosphere at low altitude (e.g., [Luo & Melrose 1995](#); [Gil et al. 2004](#)). While the radio wave propagates in the magnetosphere, it interacts with the less-dense plasma. Two eigen polarization modes of the radiation exist in this magnetized low-density plasma ([Wang et al. 2010](#)), and one of them at a certain frequency would be absorbed by the plasma via the cyclotron resonance effect ([Rafikov & Goldreich 2005](#)).

We conjecture that coherent re-emission in the cyclotron resonance region could result in giant pulses, leading to pulsars with giant pulses being located in certain regions of the P - \dot{P} diagram. This paper

is organized as follows: cyclotron resonance absorption is introduced in Section 2, and discussion and conclusion are presented in Section 3 and Section 4.

2 CYCLOTRON RESONANCE ABSORPTION

Considering a plasma with magnetic field $\mathbf{B} = (0, B_y, B_z)$ in rectangular coordinates, radiation with wave vector \mathbf{k} propagating along the z -axis ($\hat{\mathbf{k}} = \hat{\mathbf{e}}_z$) has two eigenmodes,

$$k_{R(L)} = \frac{\omega}{c} \left[1 - \frac{\omega_p^2}{\omega^2} \frac{1}{1 - \frac{1}{2} \frac{\omega_y^2}{\omega^2 - \omega_p^2} \mp \sqrt{\frac{\omega_z^2}{\omega^2} + \left(\frac{1}{2} \frac{\omega_y^2}{\omega^2 - \omega_p^2} \right)^2}} \right]^{\frac{1}{2}}, \quad (1)$$

$$\omega_y = \frac{B_y}{B} \omega_B, \quad \omega_z = \frac{B_z}{B} \omega_B,$$

where ω is the circular frequency of the radiation, $\omega_p = \sqrt{\frac{4\pi n_p q_p^2}{m_p}}$ is the plasma frequency, $\omega_B = \frac{B q_p}{m_p c}$ is the cyclotron frequency, $B = |\mathbf{B}| = \sqrt{B_y^2 + B_z^2}$ are the strength of the magnetic field, m_p and q_p are the mass and the charge of the particles in plasma, n_p is the number density of the particles, and c is the speed of light. In fact, either of the two eigenmodes is an elliptical polarization mode, and the subscript of the wave vector R(L) refers to the wave, being a right (left) circularly polarized wave for positive B_z . The electric field of the wave $\mathbf{E} = (E_x, E_y, E_z)$ for the two eigenmodes follows

$$E_{y, R(L)} = i \frac{\omega_z}{\omega} \frac{1}{1 - \frac{1}{2} \frac{\omega_y^2}{\omega^2 - \omega_{pe}^2} \pm \sqrt{\frac{\omega_z^2}{\omega^2} + \left(\frac{1}{2} \frac{\omega_y^2}{\omega^2 - \omega_{pe}^2} \right)^2}} E_{x, R(L)}. \quad (2)$$

The frequency of observed radiation is always higher than the local plasma frequency in the magnetosphere of the pulsar, which decreases along the radiation propagating path. With Eq. 1, the L-mode wave can always freely propagate, while the wave vector of the R-mode wave may take on an imaginary value for some magnetic fields, where the radiation frequency is close to the cyclotron frequency. In fact, the local plasma frequency is very low during the absorption process, the two eigenmodes change little with Eq. 2. Then the absorbed component remains unchanged. With the above assumptions, the optical depth τ of the R-mode wave can be calculated,

$$\tau \approx -\pi^2 n_p q_p \frac{1 + \frac{2\omega_{cz}^2}{\omega_{cy}^2}}{\left(1 + \frac{\omega_{cz}^2}{\omega_{cy}^2}\right)^{\frac{3}{2}}} \frac{1}{\frac{dB_y}{dz}}. \quad (3)$$

In fact, the term $\left(1 + \frac{2\omega_{cz}^2}{\omega_{cy}^2}\right) / \left(1 + \frac{\omega_{cz}^2}{\omega_{cy}^2}\right)^{\frac{3}{2}}$ is approximately 1 for $\frac{B_z}{B_y} < 3.73$, i.e., the induced angle between $\hat{\mathbf{e}}_z$ and $\hat{\mathbf{B}}$ is less than 75° , which can be always satisfied at the absorbing location. Considering a dipole field $B_y \sim B \sim \frac{\mu}{r^3}$ (where r is the distance between the pulsar center and the absorption point, μ is the magnetic dipole moment of the pulsar), a particle charge density $n_p q_p = \lambda \rho_{GJ} = \lambda \frac{B}{Pc}$ (where λ is

the ratio of the particle charge density and the GJ charge density given in Goldreich and Julian 1969, P is the period of the pulsar), Eq 3 can be expressed as below,

$$\tau \sim \frac{\pi^2 \lambda}{3cP} \left(\frac{q_p \mu}{\omega m_p c} \right)^{\frac{1}{3}}$$

$$\approx 0.155 \lambda \times \left(\frac{P}{1 \text{ s}} \right)^{-\frac{5}{6}} \left(\frac{\dot{P}}{10^{-14} \text{ s} \cdot \text{s}^{-1}} \right)^{\frac{1}{6}} \left(\frac{\nu}{1 \text{ GHz}} \right)^{-\frac{1}{3}} \quad (\text{for electrons}), \quad (4)$$

$$\approx 0.0127 \lambda \times \left(\frac{P}{1 \text{ s}} \right)^{-\frac{5}{6}} \left(\frac{\dot{P}}{10^{-14} \text{ s} \cdot \text{s}^{-1}} \right)^{\frac{1}{6}} \left(\frac{\nu}{1 \text{ GHz}} \right)^{-\frac{1}{3}} \quad (\text{for protons}). \quad (5)$$

The parameter λ can be either larger than 1 (e.g., the case of incomplete charge separation, or the case of outward particle flow) or less (e.g., in the gap).

If the optical depth is larger than 1, the radiation will be absorbed significantly. Thus a boundary can be defined according to the optical depth of 1. Some boundaries are drawn on the P - \dot{P} diagram in Figure. 1. The red stars represent the pulsars with giant pulses, whereas the blue stars represent those with giant micropulses (Cairns 2004, they are also called type II giant pulses in Wang et al. 2019). In the figure, lines with different parameters, e.g. radiation frequency ω , ratio factor λ , for electrons and protons are drawn. Coincidentally, some of these boundaries can be used to distinguish pulsars with observable giant pulses from other pulsars. Therefore, it can be speculated that the cyclotron resonance absorption may re-emit the giant pulse. As demonstrated in Figure. 1, both the electrons and protons can be the proper absorber.

3 DISCUSSION

The absorbed energy can be converted into coherent radiation and re-emitted. The radiation mechanism may be cyclotron resonance (Wang et al. 2019) or cyclotron-Cherenkov resonance (Lyutikov et al. 1999), or some other process. If the radiation turns into the observed giant pulse, the time scale of the emission should be limited. Hankins et al. (2003) found that the giant pulse of the Crab pulsar has nanosecond structure, which means that the radiation time scale should be at the nanosecond level. It requires a high radiant power. As the radiation power of a giant pulse is extraordinarily stronger than that of the normal pulses, the emission rate of giant pulses must be larger than the absorption rate of cyclotron resonance. Therefore, the radiation of a giant pulse should be energy released after its accumulation via cyclotron resonance absorption over some period. It should be an unstable process which may be related to the phenomenon of self organized criticality, which can explain the power-law flux distribution of giant pulses (Popov & Stappers 2007).

It is known that the giant pulses in some pulsars are in phase or slightly offset in phase with the high energy non-thermal radiation, such as the Crab pulsar (PSR B0531+21, Abdo 2010), PSR B1937+21 (Cusumano et al. 2003); for some pulsars, only part of the giant pulses are in phase with the

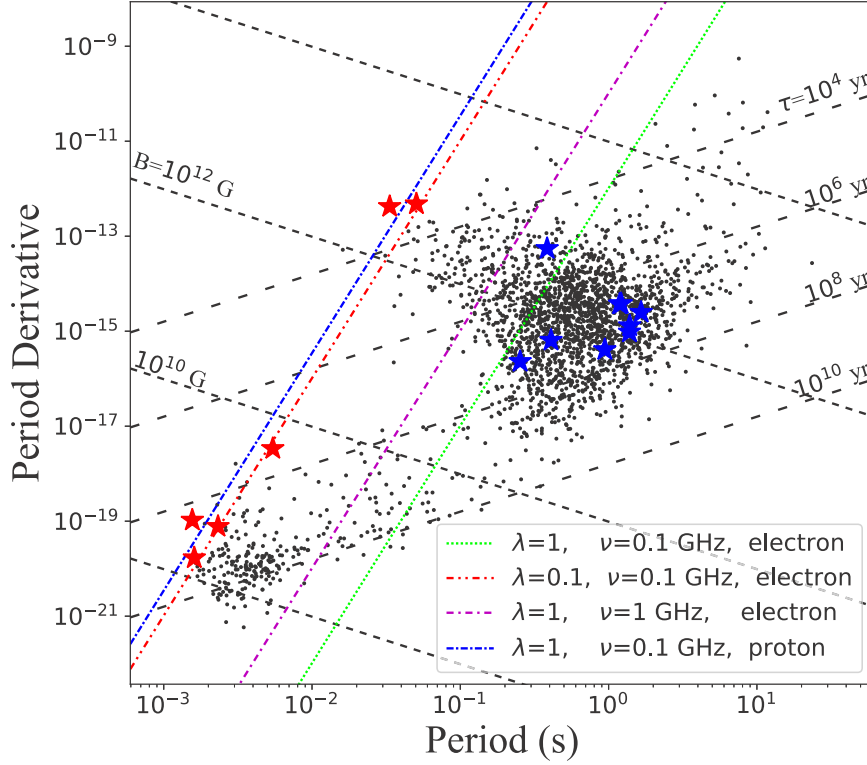


Fig. 1 The pulsars with giant pulses are marked on the P - \dot{P} diagram, where the red and blue stars represent the pulsars with giant pulses and giant micropulses, respectively. The dotted, dash-dotted and dash-dot-dotted lines mark the boundaries $\tau = 1$ for different parameters, where the red line is the reference calculated for electrons with $\lambda = 1$, $\nu = 0.1$ GHz, and the blue, magenta and green lines change with the λ , ν and particles respectively.

high energy non-thermal radiation, such as PSR B1957+20 (Main et al. 2017; Guillemot et al. 2012); for the other pulsars, the peak position at high energy band and the giant radio pulses are separated, such as PSR B1821–24A (Johnson et al. 2013) and PSR B0540–69 (Johnston et al. 2004). On the other hand, the giant pulses from Crab pulsar has no significant correlation with the X-ray radiation (Hitomi Collaboration et al. 2018), it means that the giant pulses and X-ray radiation of Crab pulsar may have different spatial origination. It should be noted that the pulse phase are always related to the radiation altitude in the dipole field, therefore the numerous observations implicate that the giant pulse and high energy non-thermal radiation may have similar radiation altitude. The X-ray radiation of Crab pulsar can be reconstructed in both slot gap (Harding et al. 2008) and annular gap model (Du et al. 2012), and radiation altitudes are both high. In fact, the cyclotron resonance occurs when the cyclotron frequency is similar to the radiation frequency and

always takes place in the high altitude region. Thus the giant pulse can have similar radiation phase to the high energy radiation.

Hankins et al. (2016) found zebra-pattern-like spectral bands in giant pulses of inter pulses from the Crab pulsar. It is worth noting that those spectral bands were only observed above 5 GHz, and all the giant pulses observed above 5 GHz exhibited the zebra-pattern-like bands. This critical frequency implies that there is a physical limit, and the frequency of cyclotron absorption may be one answer. Based on the lines in Figure 1, this speculation prefers the absorber to be the electron, or to be the protons when the λ parameter is bigger than 1 in the large outwards particle flow.

Wang et al. (2019) pointed out that the pulsars with giant pulses have a similar magnetic field at the light cylinder, which implies that the giant pulses may be generated near the light cylinder. Lyubarsky (2019) and Philippov et al. (2019) also build models that the magnetic reconnection near light cylinder can lead to radio nano-shots. In fact, the Eq. 3 can be rewritten as the following,

$$\tau \approx \frac{\pi\lambda}{6} \left(\frac{q_p}{\omega m_p c} \right)^{\frac{1}{3}} B_{LC}^{\frac{1}{3}}, \quad (6)$$

where $B_{LC} = \left(\frac{2\pi}{cP} \right)^3 \mu$ is close to the magnetic field strength at the light cylinder. This means that the boundary for the optical depth of the R-mode wave can be expressed in terms of the magnetic field at the light cylinder. So the giant pulses can also be generated from the inner region instead of near the light cylinder based on the locations of pulsars with giant pulses in the $P-\dot{P}$ diagram.

The magnetic field of any pulsar is always twisted due to the pulsar rotation. Then the drift velocity of the particles in the magnetosphere which runs parallel to the local Poynting vector must have a radial component. The Poynting vector of a dipole rotator generally points outwards, thus the particles in the magnetosphere tend to move outwards. As magnetic field distortion is more significant in the outer location, the loss of particles becomes more serious. Therefore, the particle charge density may deviate more from the GJ charge density by being farther from the pulsar, and λ becomes smaller. For the electron absorption, the magnetic field is $\sim 10^3$ G, which is almost the value at the light cylinder, indicating that the λ is smaller than 1. Whereas, for the proton absorption, the magnetic field is $\sim 10^6$ G, and the parameter λ should be bigger.

With Eq. 2, the polarization degree of each mode can be calculated. It is found that the circular polarization degree of each mode in the absorption region is very high. If the R-mode wave is absorbed, the left radiation containing only the L-mode component should be highly circularly polarized. However, the circular polarization of radiation from some pulsars with giant pulses is relatively low, e.g. the radiation from the Crab pulsar (Moffett & Hankins 1999) and PSR B1937+21 (Dai et al. 2015). This may result from the difference between the core (the region surrounded by the critical field line) and the annular region (the region between the critical field line and the last opening field line). The annular region may be free of plasma, and allow radiation to propagate freely (Du et al. 2010, 2012), while the core region may be filled

by charged particles. The radiation of normal pulses can be generated from the annular region, while giant pulses come from the core region.

4 SUMMARY

To summarize, cyclotron resonance absorption is a possible power source for the giant pulse, that might naturally explain the distribution of pulsars with giant pulses on the $P-\dot{P}$ diagram. The radiation mechanism producing giant pulses is not discussed in detail in this article, and none of the properties of giant pulses (short time duration and high power, nano-shot structure, polarization) are addressed in this model; it will be studied in the future.

In this paper, giant pulses of radio pulsars are investigated from a theoretical point of view, which could be applicable to future observational investigations. It is worth noting that, with superior sensitivity compared to any other single-dish radio telescope, Chinese FAST may help in the study of giant pulses. We would then anticipate a FAST era of pulsar science to come (Peng et al. 2000a,b; Jiang et al. 2019; Wang, Qiao, et al. 2019; Lu et al. 2020).

Acknowledgements This work is supported by the National Key R&D Program of China under grant number 2018YFA0404703, NSFCChina (Grant Nos. 11673002 and U1531243), and the Open Project Program of the Key Laboratory of FAST, NAOC, Chinese Academy of Sciences. J.G. Lu acknowledges the support of the FAST FELLOWSHIP from Special Funding budgeted and administrated by the Center for Astronomical Mega Science, Chinese Academy of Sciences (CAMS). B. Peng acknowledge the CAS-MPG LEGACY funding “Low-Frequency Gravitational Wave Astronomy and Gravitational Physics in Space”. Thanks Richard Strom for giving suggestions on the revision.

References

- Abdo, A. A., Ackermann, M., Ajello, M., et al. 2010, ApJ, 708, 1254 3
- Cairns, I. H. 2004, ApJ, 610, 948 3
- Cusumano, G., Hermsen, W., Kramer, M., et al. 2003, A&A, 410, L9 3
- Dai, S., Hobbs, G., Manchester, R. N., et al. 2015, MNRAS, 449, 3223 5
- Du, Y. J., Qiao, G. J., Han, J. L., et al. 2010, MNRAS, 406, 2671 5
- Du, Y. J., Qiao, G. J., & Wang, W. 2012, ApJ, 748, 84 4, 5
- Gil, J., Lyubarsky, Y., & Melikidze, G. I. 2004, ApJ, 600, 872 1
- Goldreich, P. & Julian, W. H. 1969, ApJ, 157, 869 3
- Guillemot, L., Johnson, T. J., Venter, C., et al. 2012, ApJ, 744, 33 4
- Hankins, T. H., Kern, J. S., Weatherall, J. C., et al. 2003, Nature, 422, 141 3
- Hankins, T. H., Eilek, J. A., & Jones, G. 2016, ApJ, 833, 47 5

- Harding, A. K., Stern, J. V., Dyks, J., et al. 2008, *ApJ*, 680, 1378 [4](#)
- Hitomi Collaboration, Aharonian, F., Akamatsu, H., et al. 2018, *PASJ*, 70, 15 [4](#)
- Jiang, P., Yue, Y. L., Gan, H. Q., et al. 2019, *Sci. China-Phys. Mech. Astron.*, 62, 959502 [6](#)
- Johnston, S., Romani, R. W., Marshall, F. E., et al. 2004, *MNRAS*, 355, 31 [4](#)
- Johnson, T. J., Guillemot, L., Kerr, M., et al. 2013, *ApJ*, 778, 106 [4](#)
- Lu, J. G., Li, K. J. and Xu, R. X. 2020, *Sci. China-Phys. Mech. Astron.*, 63, 229531 [6](#)
- Luo, Q., & Melrose, D. B. 1995, *MNRAS*, 276, 372 [1](#)
- Lyubarsky, Y. 2019, *MNRAS*, 483, 1731 [5](#)
- Lyutikov, M., Blandford, R. D., & Machabeli, G. 1999, *MNRAS*, 305, 338 [3](#)
- Main, R., van Kerkwijk, M., Pen, U.-L., et al. 2017, *ApJ*, 840, L15 [4](#)
- Moffett, D. A. & Hankins, T. H., 1999, *ApJ*, 522, 1046 [5](#)
- Peng, B., Strom, R. G., Nan, R. et al. 2000, *Perspectives on Radio Astronomy: Science with Large Antenna Arrays*, 25 [6](#)
- Peng, B., Nan, R., & Su, Y. 2000, *Proc. SPIE*, 45 [6](#)
- Philippov, A., Uzdensky, D. A., Spitkovsky, A., et al. 2019, *ApJ*, 876, L6 [5](#)
- Popov, M. V., & Stappers, B. 2007, *A&A*, 470, 1003 [3](#)
- Rafikov, R. R., & Goldreich, P. 2005, *ApJ*, 631, 488 [1](#)
- Wang, C., Lai, D., & Han, J. 2010, *MNRAS*, 403, 569 [1](#)
- Wang, H., Qiao, G. J., Du, Y. J., et al. 2019, *RAA*, 19, 21 [6](#)
- Wang, W., Lu, J., Zhang, S., et al. 2019, *Sci. China-Phys. Mech. Astron.*, 62, 979511 [3](#), [5](#)